Drug Development and Industrial Pharmacy, 22(1), 67–75 (1996)

The Viscoelastic Deformation of Some Tableting Materials as Assessed by Indentation Rheology

Metin Çelik[1] and Michael E. Aulton[2]

[1]*Pharmaceutical Compaction Research Laboratory and Information Center, College of Pharmacy, Rutgers University, P.O. Box 789, Piscataway, NJ 08855-0789*
[2]*Department of Pharmaceutical Sciences, De Montfort University, Leicester LE1 9BH, United Kingdom*

ABSTRACT

The time-dependent deformation of compacts prepared from four tablet compression bases has been assessed by microindentation rheology. Compacts were made from Avicel PH101, Emcompress, Emdex, and Starch 1500 at compaction pressures of 30, 60, and 90 MPa. A spherical indenter, 1.55 mm diameter, was allowed to indent into the compacts under a fixed load of 5.89 N (600 g) and the changing depth of indentation was recorded. The corresponding creep compliance versus time curve was calculated and analyzed by discrete mechanical analysis to yield Maxwell and Voigt "spring and dashpot" mechanical models. This yielded quantitative data on instantaneous elastic compliance and modulus, the time-dependent viscoelastic compliances, viscosities, and retardation times of each Voigt unit, and the Newtonian viscosity of the compacts. In general, the deformation of the compacts was in the rank order Starch 1500 > Avicel PH101 > Emdex > Emcompress. Emcompress showed negligible viscoelasticity and plasticity. For the other compacts, the number of Voigt units (a reflection of the magnitude of viscoelasticity) generally decreased with increasing compaction pressure between 30 and 90 MPa. For example, Avicel PH101 compacts required five Voigt units to define their deformation when compressed at 30 MPa, three at 60 MPa and two at 90 MPa. The corresponding numbers for Emdex compacts were 4, 3, and 2, while Starch 1500 compacts showed a high degree of viscoelasticity at high compaction pressure, exhibiting 5 (at 30 MPa), 4 (at 60 MPa), and still 4 Voigt units even at 90 MPa compaction pressure. The rank order for the viscosity values was Starch 1500 < Avicel PH101 < Emdex << Emcompress compacts. Long-term

indentation rheology proved to be a valuable tool in assessing the viscoelastic characteristics of pharmaceutical compacts and will be useful in predicting time-dependent scale-up problems during the change from single-punch development presses to high-speed rotary production machines.

INTRODUCTION

It is possible to evaluate the tableting characteristics of pharmaceutical materials by examining their time-dependent strain movements occurring during compression and after ejection. One of the methods of assessing these properties is the indentation rheology, which involves following the changes in depth of penetration of a loaded indenter into preformed tablets. The most common pharmaceutical use of indentation testing is to determine the quasistatic hardness of tablets and crystals. Hardness is a measure of the resistance to local permanent deformation (1). Standard hardness testing involves penetration of a loaded indenter into the test specimen for a relatively short time, typically between 10 and 30 seconds. This short period may be sufficient for metals to complete their deformation; however, it was shown by Aulton and Tebby (2) that, for many pharmaceutical compacts, indentation is far from complete after this time. In their work, maximum penetration times were recorded as 1.32 ks and 6.72 ks for Emcompress and Emdex, respectively. They also found an empirical rank-order relationship between the compression characteristics of a number of tablet bases and the ratio of the time of penetration of a spherical indenter under load to the time of relaxation after load removal. It is possible to quantify and characterize the viscoelastic properties of the material by application of a mathematical analysis of the creep curve obtained from the test. The various methods of analyzing creep curves have been reviewed by Barry (3). One of these was used in this paper.

Creep Analysis

Of the various methods available to examine viscoelastic behavior, the most important one, which has been used for many materials, is the creep test. In the creep test, a stress (s_0) is applied abruptly to the sample at $t = 0$ and held constant while the strain (e) is observed as a function of time. The experimental conditions may be defined as

$$t < 0, \quad \sigma = 0$$

$$t \geq 0, \quad \sigma = \sigma_0$$

The creep compliance at any time, $J_c(t)$, for material is defined as the strain at time t divided by the applied stress at time t. Thus for $t \geq 0$

$$J_c(t) = \varepsilon(t)/\sigma_0 \tag{1}$$

Discrete Spectral Analysis

A typical creep curve for a linear viscoelastic material is shown in Figure 1. According to convention, the curve is in units of compliance (strain/stress) versus time; thus, the same curve is produced regardless of the magnitude of the applied stress and the method of measurement of strain, provided that the test is run until the linear viscoelastic region is reached. The viscoelastic behavior can be represented in the form of a mechanical model that consists of a Maxwell unit (a spring and dashpot in series) in series with several Voigt units (each of which is a spring and dashpot in parallel). For the case where three Voigt units are required, the creep compliance can be defined by equation

$$J_c(t) = J_0 + \sum_{i=1}^{3} J_i[1 - \exp(-t/T)] + t/\eta_N \tag{2}$$

$J_c(t)$ represents the total creep compliance at any time t and it is a nondecreasing function of time with the di-

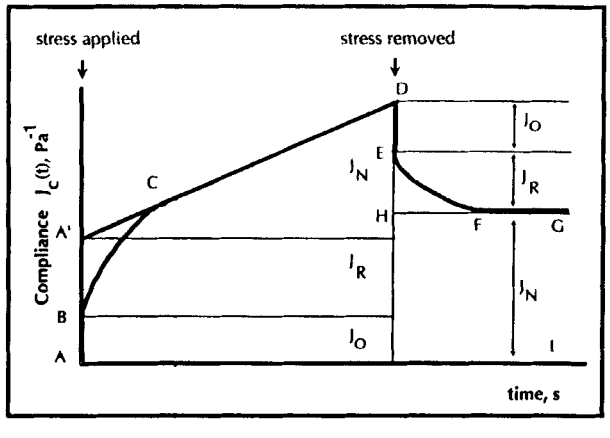

Figure 1. A typical creep compliance curve. (After Sherman, 1970.)

mensions of a reciprocal modulus, typical units being $(MPa)^{-1}$.

J_0 is the initial elastic compliance obtained by dividing the instantaneous elastic strain (measured at the onset of the applied stress) by the applied stress. In the mechanical model, J_0 is the compliance of the spring that represents the elastic stretching or compression of primary bonds.

J_1 to J_3 are the compliances of Voigt units 1 to 3, respectively; also they reflect the contribution of the retarded elastic region to the total compliance. T represents a retardation time which, for each Voigt unit, is given by the product of the appropriate compliance of the spring and the dynamic viscosity of the dashpot. Thus, T_1 to T_3 represent the retardation times of Voigt units 1 to 3, respectively. These units represent that part of the structure of the material under test in which secondary bonds break *and reform* during deformation. Retardation time is a function of the time required for such breakage to occur and reform. Since bonds do this at different rates, a spectrum of retardation times exists.

η_N is the residual shear viscosity represented by the dashpot of the Maxwell model. Its value is obtained from the creep curve after a long period when there is a linear region of change in compliance with time. During this part of the creep experiment, the stress has been applied for sufficient time to ensure that all the Voigt units are essentially fully deformed, when further deformation is viscous flow and is nonrecoverable. It should be appreciated that this viscous deformation begins at the onset of applied stress, i.e., $t = 0$. Because Voigt unit deformation is exponential, and thus mathematically requires infinite time, the onset of the linear region is taken to be the point at which further curvature is negligible.

Figure 1 illustrates that, in practice, the creep compliance versus time curve can be split into three separate regions, as suggested by Sherman (4).

1. A-B is the region of instantaneous recoverable elastic compliance that can be modeled as a Hookean spring.

$$J_0 = 1/G_0 = \varepsilon_0/\sigma_0 \tag{3}$$

where G_0 is the modulus of rigidity of the material, ε_0 is the instantaneous strain ($t = 0$) and σ_0 is the constant applied shear stress. J_0 is easily derived from the experimental data.

2. B-C is the time-dependent retarded elastic region with a compliance J_R. In its simplest form,

$$J_R = \varepsilon_R/\sigma_0 \tag{4}$$

where ε_R is the total strain in this region. This is the situation when the retarded elasticity is represented by a single Voigt unit. For a line spectrum containing more than one unit, a summation term is used,

$$J_R = \sum J_i[1 - \exp(-t/T_i)] \tag{5}$$

3. A'D is the linear region of Newtonian compliance, J_N, which is only visible in isolation between C-D, i.e., after the cessation of the retarded elastic deformation. Some bonds within the material rupture and flow past each other without reforming. Under these conditions,

$$J_N = t/\eta_N = \varepsilon_N(t)/\sigma_0 \tag{6}$$

where $\varepsilon_N(t)$ is the strain in the region at time t.

Removal of the stress gives the recovery curve DG. There is instantaneous elastic recovery, DE, of the same magnitude as AB (both equal to J_0), followed by retarded elastic recovery, EF, equivalent to the retarded region of the creep curve (J_R). As bonds were irreversibly broken in the A'D region of the creep curve, this part of the structure is not recovered and there is no further deformation between F and G. The vertical distance GI (equal to J_N) is equivalent to DH.

The value of J_0 in equation 2 can be obtained from the creep curve using equation 3. η_N may be obtained from the reciprocal of the slope of the linear portion of the curve using equation 6. A graphical procedure is employed to analyze the retarded elastic region (BC). In equation 5, let

$$Q = \sum J_i \exp(-t/T_i)] \tag{7}$$

so that Q represents the distance, at any time t, between the curved portion of the plot and the extrapolated linear portion (Figure 2). This step is necessary to "strip" the nonrecoverable component of the deformation from the retarded elastic component up to point C on the curve in Figure 1. The equation can be written in logarithmic form, dropping the summation sign, as

$$\ln Q = \ln J_i - t/T_i \tag{8}$$

When ln Q is plotted against time, as illustrated in Figure 2b, a straight line results at large values of t. Consideration of equation 8 indicates that the slope of the linear region is the inverse of a retardation time T and the intercept of the extrapolated linear region on the ordinate provides a compliance J_1. For short time values the data are not linear. This indicates the presence of more than one Voigt unit. The magnitudes of a second retardation time, T_2 and J_2 are obtained by plotting

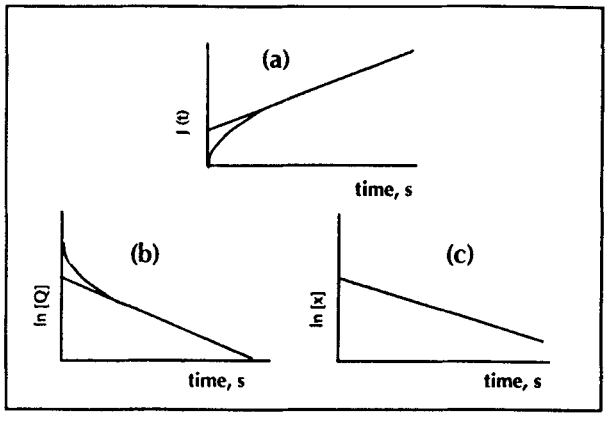

Figure 2. A graphical procedure employed to analyze retarded elastic region of a creep compliance curve ($[x] = \ln[Q - J_1 \exp(-t/T_i)]$).

$\ln[Q - J_i \exp(-t/T_i)]$ against t. Values may be obtained from the distance between the extrapolated linear region and the curved portion of the ln Q versus t plot. A linear portion is again obtained and values of compliance J_3 and T_3 are derived from the curved part of the plot as before. The appropriate values for viscosities are obtained from the following relationship:

$$\eta_i = T_i/J_i \quad (9)$$

The process is repeated, resulting in

$$[\ln(Q - J_1 \exp(-t/T_1) - J_2 \exp(-t/T_2) \cdots]$$

The logarithm of the difference is plotted against time, t, until a linear relationship results (Figure 2c).

MATERIALS AND METHODS

Materials

The compression bases used in this study were microcrystalline cellulose (Avicel PH101, FMC Corporation), dicalcium phosphate dihydrate (Emcompress, Mendell), dextrates (Emdex, Mendell), and modified starch (Starch 1500, Colorcon). All materials were compressed following storage at 40–60°C for 12–18 hours and without lubrication.

Compaction

Using a programmable high-speed Mayes Universal Hydraulic Testing Machine, compacts, 25.4 mm diameter and nominally 12 mm thickness, were compressed from Avicel PH101, Emcompress, Emdex, and Starch 1500 at compaction pressures of 30, 60, and 90 MPa.

Indentation Testing

The determination of the indentation profile is based on the accurate measurement of very small changes in the vertical displacement of the indenter tip, normal to the specimen surface. The details of the indenter are reported elsewhere (5).

The apparatus of White and Aulton was used, in which a load of 600 g (5.89 N) was applied to a spherical sapphire indenter of diameter 1.59 mm. Indenter movement was followed by a displacement transducer (Sangamo Weston Control, 2 mm, AC type), the signal being amplified by a Sangamo C-56 transducer meter. The amplified signals that ranged from 0 to 10 V were passed to a negative differential amplifier to produce 0 to 200 mV voltages. The "reduced" analogue voltages (0–200 mV) were fed into the 3D analogue to digital converter, which in turn converted the output voltages into digital form for the IEEE interface of a PC. The transducer was calibrated using a Shardlow micrometer (0–25 mm travel, 65 mm drum).

In order to measure the indentation profile of a given compact, the static height of the indenter shaft assembly was adjusted so that the sphere rested lightly in contact with the compact surface. Once the height of the shaft was correctly set, the transducer was adjusted to produce a logged byte value within the working range of 0.5 mm. The transducer was then fixed firmly in position by means of two locking screws.

Indentation tests were performed by following, over a long period, the depth of penetration of the spherical indenter into the surface of the compacts prepared. After load application, changes in the depth of indentation were recorded for up to 20 ks using software developed by the author. The data captured by the computer were stored on disks for future data evaluation. A suite of software was developed to analyze the data obtained from the above techniques.

RESULTS AND DISCUSSION

Creep Compliance Plots

There is an obvious analytic problem with spherical indentation in that although the applied load is constant, the stress beneath the indenter is continually decreasing

as the indenter penetrates into the sample, and thus the area of indentation increases. The problem of the partial penetration of an incompressible semi-infinite plane viscoelastic surface by a smooth rigid sphere has been solved by using the following equation (6):

$$J_c(t) = (16/3) * R^{1/2} * (1/F) * h(t)^{3/2} \quad (10)$$

where $J_c(t)$ is the creep compliance at time t, R is the radius of indenting sphere, F is the indentation load, and $h(t)$ is the depth of indentation at time t. This equation was used in the calculations of creep compliance for indentation data. The values of R and F were 0.795 mm and 5.89 N, respectively, in this work.

Visual Evaluation of the Creep Compliance Curves

Graphs of creep compliance for the indentation of compacts of the three materials tested are shown in Figures 3a, b, and c. The results for Avicel PH101, Emcompress, Emdex, and Starch 1500 compacts are shown on each graph for 30 MPa (Figure 3a), 60 MPa (Figure 3b), and 90 MPa (Figure 3c) compaction pressures.

Emcompress compacts showed the largest initial elastic deformation of the four bases studied, but then exhibited the least subsequent time-dependent strain. During indentation, further penetration became insignificant after about 0.5 s. This may be explained in terms of the known brittle nature of Emcompress. The deformation of this material was too small to enable a creep analysis to be performed. The deformation of Emcompress compact appeared to have little dependence on compaction pressure, as shown by the results obtained from both techniques.

In all cases Emdex compacts showed a greater degree of time-dependent deformation than Emcompress compacts. This was reflected both in the total actual deformation and the time required to complete the majority of the deformation.

Avicel PH101 and Starch 1500 compacts showed similar deformation and in all cases this time-dependent viscoelastic deformation was greater than that observed for Emdex and Emcompress compacts. The rank order for their deformation was found to be pressure dependent. This could be due to the pressure-dependent properties of Avicel PH101 reported by Sixsmith (7).

An interesting and clear observation of the deformation behavior of Avicel PH101 and Starch 1500 compacts can be seen when Figure 4 is examined, in which

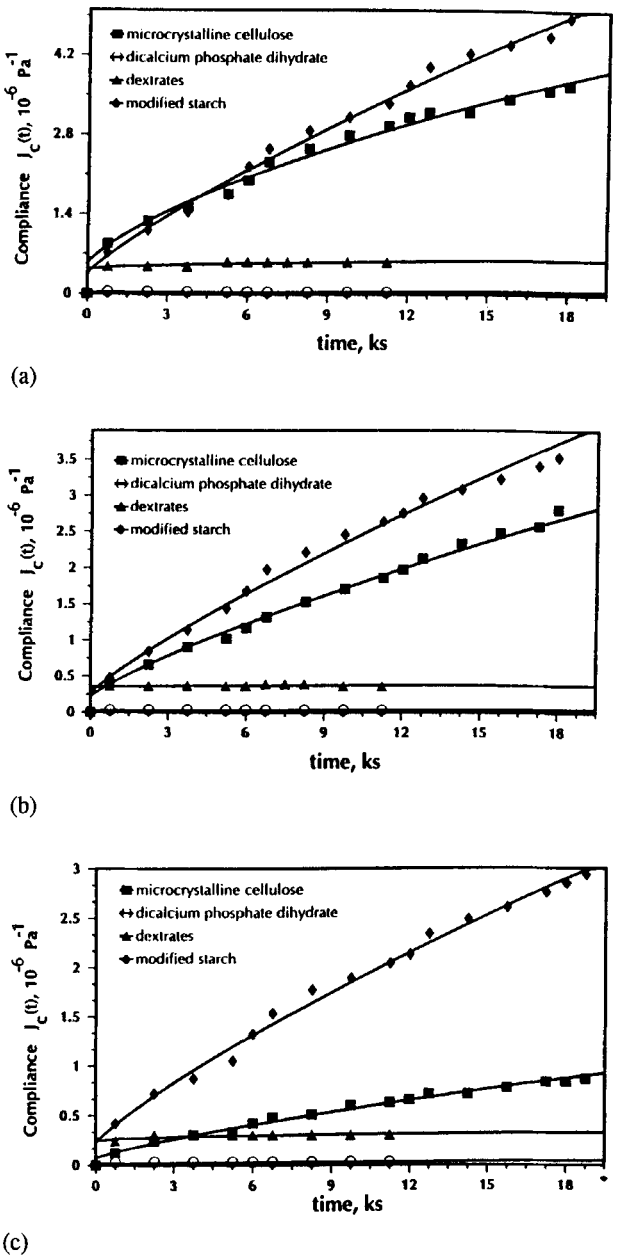

Figure 3. Creep compliance versus time plots for the compacts made at (a) 30 MPa, (b) 60 Mpa, and (c) 90 MPa.

the creep compliances at various times are plotted against compaction pressure for these two materials. The difference between creep compliances for indentation at 10 ks and 20 ks for both materials indicates the importance of the duration of test involved. It can be suggested that a long-term indentation gives more meaningful results than a short-term one. This is further proven

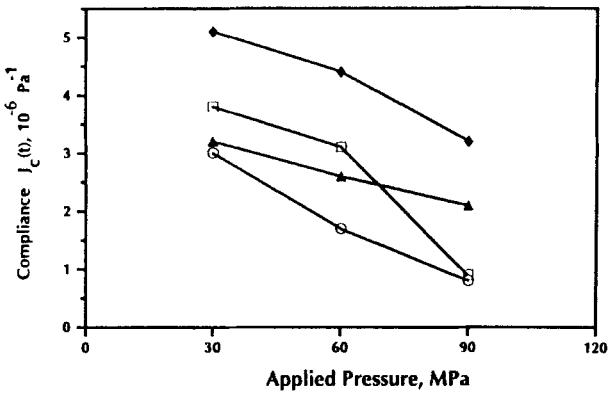

Figure 4. A comparison of creep compliance versus compaction pressure for the compacts of microcrystalline cellulose (○,□) and modified starch (▲,◆) after 10 ks (○,▲) and 20 ks (◆,□) indentation.

by examining the initial part of the creep compliance versus time plots for indentation—for example, Emdex compressed at 60 MPa exhibited the maximum indentation up to 1 ks, but after this period, Avicel PH101 and Starch 1500 compacts showed greater penetration of the indenter than did Emdex compacts. Therefore, the information obtained from a short-term indentation test may mislead the observer about the true viscoelastic properties of the compacts.

The interesting finding is that, in all cases, Starch 1500 and Avicel PH101 compacts exhibited less deformation with increasing compaction pressure, suggesting that their compact properties are dependent on compaction pressure. However, Avicel PH101 exhibited a greater rate of dependency on compaction pressure, producing increasingly less deformation with increasing pressure if compared with Starch 1500 compacts. This also supports the pressure-dependent properties of Avicel discussed earlier.

Starch 1500 compacts usually showed higher creep compliance than exhibited by Avicel PH101 compacts and the difference became greater when the indentation time was prolonged from 10 ks to 20 ks.

Discrete Spectral Analysis of Creep Compliance Curves

In addition to the visual comparison of the curves of creep occurring both during and after compression, it was also possible to characterize the deformation of the material by using Maxwell and Voigt models and creep analysis. In order to obtain a number of models for each sample individually, discrete spectral analysis, which has been described earlier, was applied to the data of that sample by using a specially developed software program.

An analysis program was written to plot creep compliance versus time plots for indentation. In this program, time values for the linear section of the plots were fed into the computer to execute a regression analysis in order to determine the slope of linear section of the curve. The reciprocal of the slope gives the viscosity of the material (η_N) in accordance with equation 6. The J_0 values were taken as experimentally determined creep compliance values for indentation at $t = 0.5$ s.

The above analysis program was also used first to print $\ln(Q_i)$ versus time plots. A typical series of these logarithmic plots is given in Figure 5 (a, b, and c) for

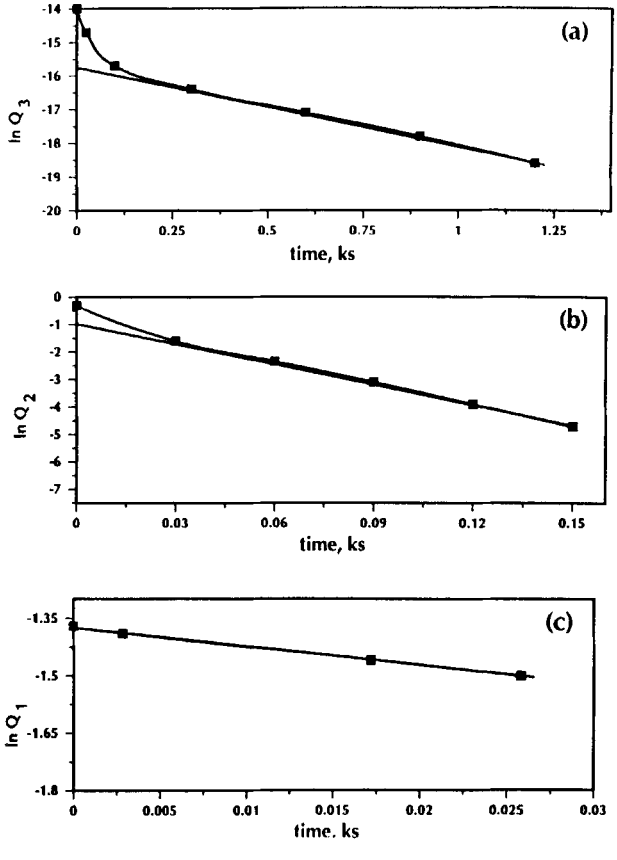

Figure 5. Discrete spectral analysis of creep compliance (three Voigt models [$I = 3$]) for the dextrate compacts made at 60 MPa.

the case of Emdex compacts. The y-axis intercept value of the extrapolated linear region and slope of this linear section were calculated and were used to determine J_i, T_i, and η_i.

It was not possible to apply this analysis for Emcompress compacts because of the insignificant magnitude of time-dependent strain of compacts of this material and obvious lack of viscoelasticity compared to the other compacts.

The model representations of the viscoelastic behavior of the compacts examined (as determined by the above analysis method) are shown in Figure 6 (a, b, and c). The number of Voigt models given by the indentation test for a given compact appeared to be dependent on the applied pressure. All the bases examined exhibited less Voigt elements in the models with increased compaction pressure, suggesting that high compaction pressure produced more restricted deformation. This was also observed on visual comparison of the creep compliance curves as mentioned above.

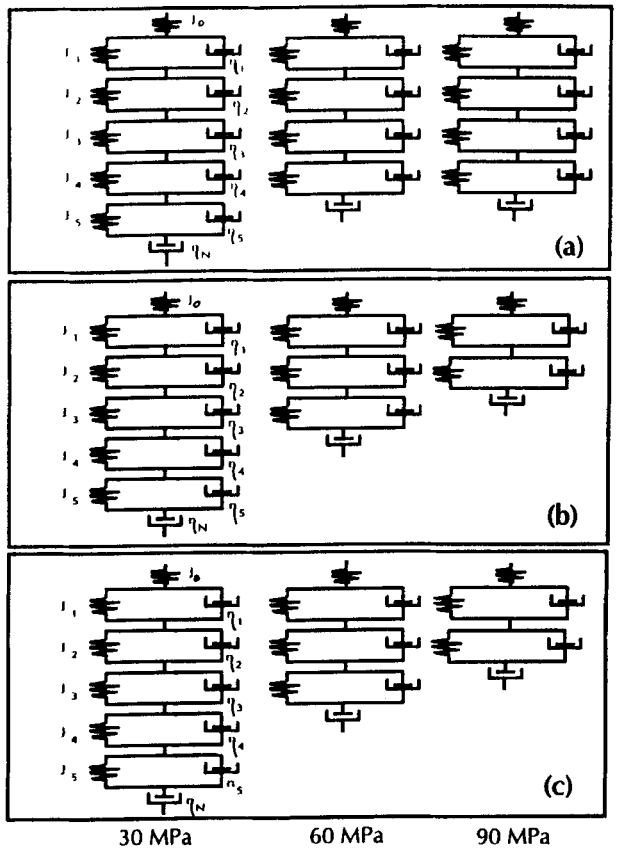

Figure 6. Voigt models for compacts of modified starch (a), microcrystalline cellulose (b), and dextrates (c) compressed at 30, 60, and 90 Mpa.

The advantage of a study of creep compliance curves and analysis of these curves by discrete spectral analysis was that it produced both empirical and quantitative information about the properties of a given material.

Numerical values yielded by the creep analysis for Starch 1500, Avicel PH101, and Emdex compacts are shown in Table 1. It was not possible to obtain these parameters for Emcompress compacts because of their marked lack of time-dependent deformation characteristics referred to previously.

The relative magnitude of the instantaneous creep compliance J_0 confirms the comments made earlier from the data presented in Figures 3a, b, and c. Table 1 shows that J_0 is influenced by compaction pressure; all compacts showed a continued reduction in compliance with increasing compaction pressure. This reduction in compliance indicates a corresponding increase in elastic modulus of the compacts resulting from their increased rigidity brought about by the compaction process.

The rank order of the magnitudes of viscosity values (η_N) of the compacts was Starch 1500 < Avicel PH101 < Emdex. Although it could not be quantified, it could be predicted that the viscosity of the Emcompress was very much higher. A gradual increase in apparent viscosity of the compacts, as reflected in the η_N data, was observed as compaction pressure was increased. This is to be expected as higher compaction pressures produced greater consolidation of the compacts and thus greater restrictions to further deformation. The advantage of the use of indentation methodology and creep analysis is that it has enabled changes in compact properties resulting from the tableting process to be quantified, in terms of J_0 and η_N.

CONCLUSIONS

Long-term indentation rheology has proved to be a valuable tool in assessing the viscoelastic characteristic of pharmaceutical compacts. It clearly differentiated the deformation properties of the four directly compressible excipients chosen for this study and the results confirmed the known tableting characteristics of these materials. Thus, one can be confident that indentation rheol-

Table 1

Numeric Values of Viscoelastic Parameters for the Compacts of Materials Prepared at 30, 60, and 90 MPa

		Starch 1500			Avicel PH101			Emdex		
Voigt Model		30 MPa	60 MPa	90 MPa	30 MPa	60 MPa	90 MPa	30 MPa	60 MPa	90 MPa
	J_0	$8.500 * 10^{-8}$	$4.700 * 10^{-8}$	$3.800 * 10^{-8}$	$2.500 * 10^{-7}$	$6.500 * 10^{-8}$	$1.200 * 10^{-8}$	$9.800 * 10^{-8}$	$7.200 * 10^{-8}$	$6.000 * 10^{-8}$
	J_1	$7.233 * 10^{-7}$	$1.420 * 10^{-7}$	$5.495 * 10^{-7}$	$1.380 * 10^{-6}$	$1.434 * 10^{-7}$	$1.709 * 10^{-7}$	$8.600 * 10^{-8}$	$1.973 * 10^{-7}$	$9.550 * 10^{-8}$
#1	η_1	$2.186 * 10^{10}$	$2.227 * 10^{11}$	$2.785 * 10^{10}$	$1.116 * 10^{10}$	$1.126 * 10^{11}$	$2.843 * 10^{10}$	$6.315 * 10^{10}$	$4.958 * 10^{9}$	$2.307 * 10^{10}$
	T_1	$1.582 * 10^{4}$	$3.184 * 10^{4}$	$1.530 * 10^{4}$	$8.294 * 10^{4}$	$1.616 * 10^{4}$	$4.859 * 10^{3}$	$5.431 * 10^{3}$	$9.786 * 10^{2}$	$2.205 * 10^{3}$
	η_N	$4.705 * 10^{9}$	$7.949 * 10^{9}$	$8.669 * 10^{9}$	$4.610 * 10^{9}$	$7.950 * 10^{9}$	$2.453 * 10^{10}$	$1.937 * 10^{11}$	$2.010 * 10^{11}$	$2.623 * 10^{11}$

ogy could be a predictive tool for the analysis of potential scale-up problems in novel tablet formulations.

REFERENCES

1. F. P. Bowden and D. Tabor, The Friction and Lubrications of Solids, 2nd ed., part II, chapter XVI, Oxford University Press, London, 1964.
2. M. E. Aulton and H. G. Tebby, J. Pharm. Pharmacol., 28, Suppl., 66p (1976).
3. B. M. Barry, Adv. Pharm. Sci., 4, 1 (1974).
4. P. Sherman, Industrial Rheology, Academic Press, London and New York (1970).
5. P. J. P. White and M. E. Aulton, J. Phys. E. Sic., Instrum., 13, 380 (1980).
6. E. H. Lee and J. R. M. Rodok, J. Appl. Mech., 27, 438 (1960).
7. D. S. Sixsmith, J. Pharm. Pharmacol., 29, 33 (1977).